Electronic Supplementary Material (ESI) for Sustainable Energy & Fuels.

Supporting information

Cobalt Sites Coordinated Polyterthiophene Derivant/Hematite Hybrid Photoanode for Light-driven Water Oxidation

Wenhao Shang,[a†] Hao Yang,[b†] Yingzheng Li,[a] Chang Liu,[a] Ziqi Zhao,[a] Yu Shan,[a] Fei Li,[a] Licheng Sun[a,b,c] and Fusheng Li[a*]

[a] *State Key Laboratory of Fine Chemicals, Frontier Science Center for Smart Materials, Dalian University of Technology, 116024 Dalian, China. E-mail: fusheng@dlut.edu.cn*

[b] *Department of Chemistry, School of Engineering Sciences in Chemistry, Biotechnology and Health, KTH Royal Institute of Technology, 10044, Stockholm, Sweden*

[c] *Center of Artificial Photosynthesis for Solar Fuels and Department of Chemistry, School of Science and Research Center for Industries of the Future, Westlake University, 310024 Hangzhou, China*

† These authors contributed equally to this work.

Experimental Section

Materials and Reagents

Dibasic sodium phosphate (Na_2HPO_4, 99%), sodium dihydrogen phosphate (NaH_2PO_4, 99.5%), sodium nitrate ($NaNO_3$, 99%), hydrochloric acid (HCl, 37%), Cobalt acetate ($Co(CH_3COO)_2$, 99%), ferric chloride hexahydrate ($FeCl_3 \cdot 6H_2O$, 99%), ethylenediamine tetraacetic acid disodium (EDTA-2Na) were purchased from Aladdin® China. [2,2';5',2"]terthiophene-3',4'-diamine and 4,7-phenanthroline-5,6-dione were purchased from local suppliers. The high-purity water (18.2 $M\Omega \cdot cm^{-1}$) used in all tests was supplied by a Milli-Q system. Fluorine-doped tin oxide conductive glass (FTO, NGS 8 Ω 10 mm × 25 mm × 2.2 mm), all the FTO substrates in all experiments were cleaned with deionized water, ethanol and acetone by ultrasonic cleaning machine for 20 min before being used. All organic solvents were directly used without purification.

Physical Characterization

The morphology of all films was characterized by ultrahigh resolution field emission scanning electron microscopy (SEM, JSM-7900F, operated at 5 kV) and the elemental mappings were obtained from energy dispersive X-ray (EDX) microanalysis (Oxford EDS Inca Energy Coater 300). High-resolution transmission electron microscopy (HRTEM) and elemental mappings were obtained from the JEM-F200 operating at an acceleration voltage of 200 kV. The crystal information was tested by X-Ray diffractometer (XRD, Smartlab 9kW). The element valence state of films was analyzed by X-ray photoelectron spectroscopy (XPS, Thermo Fisher ESCALAB™ Xi^+). The vibration and rotation of chemical bands were investigated by micro-Raman spectra (Thermo Fisher DXR Microscope). The absorption spectra of photoanodes were taken by a solid UV-Visible (UV-vis) spectrometer (UV-3600 Plus).

Synthesis of TTh-N

The TTh-N was prepared by the method from the literature report.[1] A mixture of [2,2';5',2"] terthiophene-3',4'-diamine (143 mg, 0.51 mmol), 4,7-phenanthroline-5,6-dione (120 mg, 0.57 mmol) and 4-methylbenzenesulfonic acid (10 mg, 0.06 mmol) in EtOH (20 mL) was stirred at 80 °C for 4 h. The resulting greenish-blue powder of TTh-N (191 mg, 83%) was filtered, washed with EtOH and dried in vacuo. ^{1}H NMR (400 MHz, CD_2Cl_2/CF_3COOH): δ 9.70 (d, *J* = 8.2 Hz, 2H), 9.52 (d, *J* = 5.2 Hz, 2H), 8.57 (t, *J* = 6.3 Hz, 2H), 7.95 (d, *J* = 3.6 Hz, 2H), 7.67 (d, *J* = 5.0 Hz, 2H), 7.28 (t, *J* = 4.3 Hz, 2H). FTIR: 1623, 1421 cm^{-1} (C=C); 1590 cm^{-1} (C=N); 692 cm^{-1} (C−S); 848 cm^{-1} (C−H). HRMS: calculated m/z of $[M+H]^+$: 453.0224; found: 453.0292.

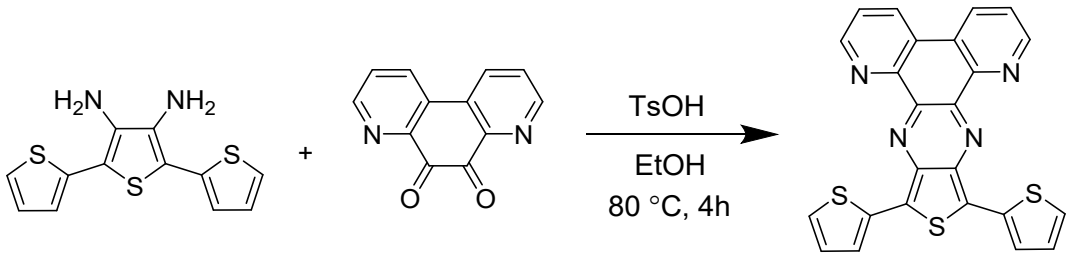

Scheme S1. Synthetic routes of TTh-N.

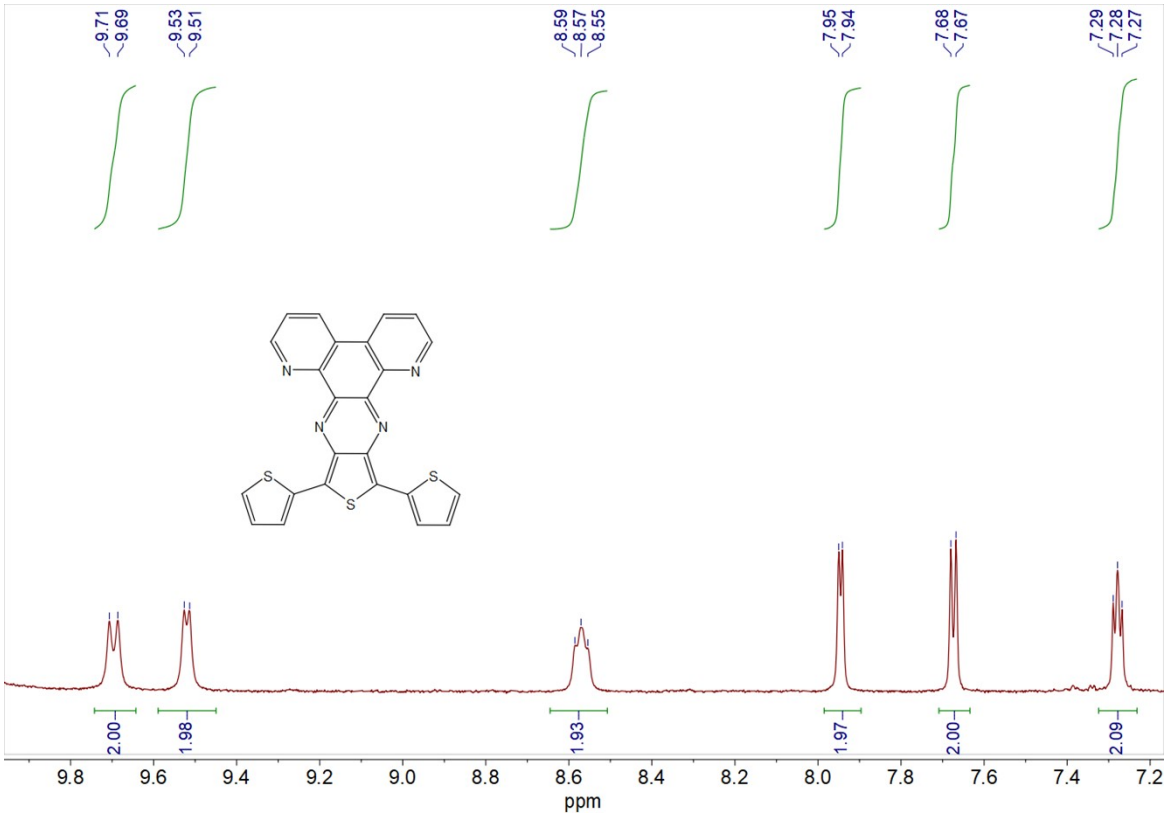

Figure S1. ^{1}H-NMR spectrum of TTh-N.

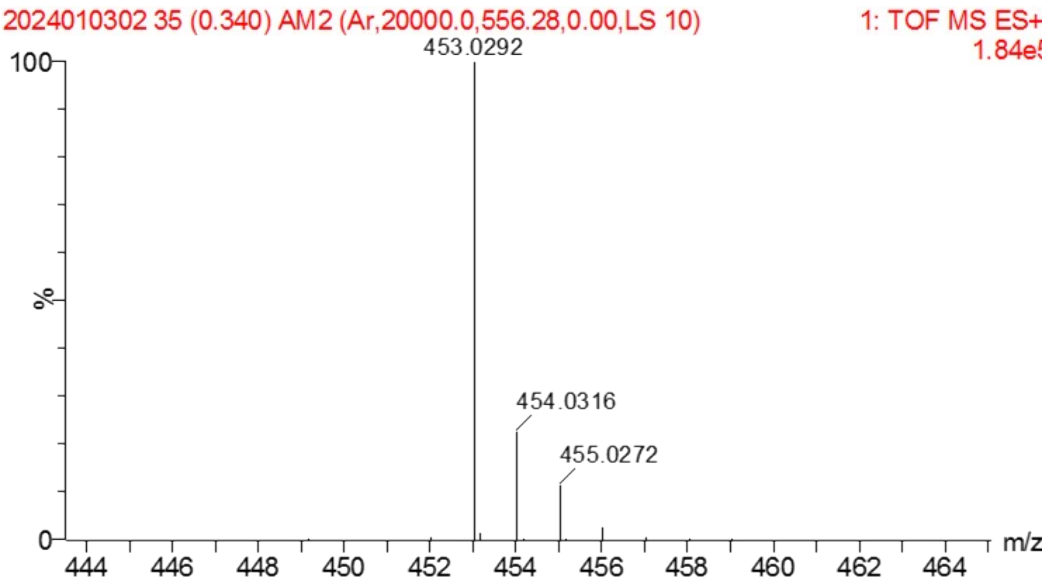

Figure S2. High-resolution mass spectrum of TTh-N.

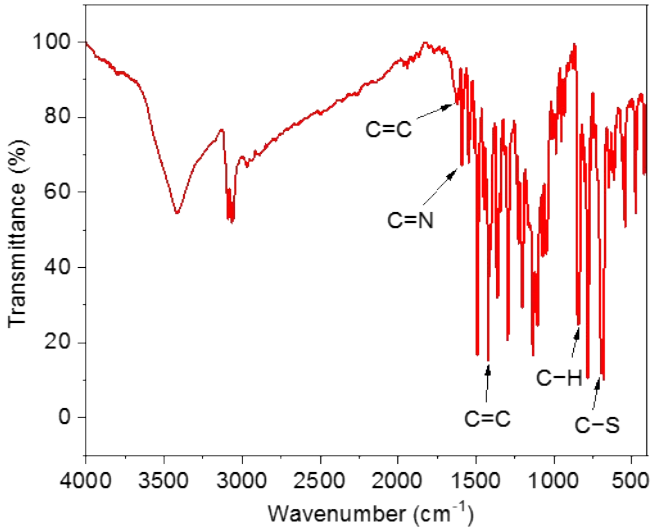

Figure S3. FT-IR spectrum of TTh-N.

Preparation of α-Fe_2O_3 photoanodes

The α-Fe_2O_3 film was prepared by a modified method from the literature report.[2] Briefly, 169.98 g of $NaNO_3$ (2 mol) and 81.04 g of $FeCl_3 \cdot 6H_2O$ (0.3 mol) were dissolved in 1 L deionized water. The pH of this solution was adjusted to 1.5. The surface of the cleaned FTO glass substrate was covered by Kapton tapes (3M) with an area of 1×1 cm^2 of the conductive side reserved. The FTO glass was

immersed into 15 mL of the above solution in a sealed glass vial. The reaction was placed in an oven at 95°C for 5 h. After that, the FeOOH nanorod films were deposited on the FTO glass substrates and washed with DI water three times before drying in air. The samples were calcinated at 800 °C in the air for 10 min (ramping rate 15 °C/min) to obtain α-Fe_2O_3 thin film photoanodes.

Preparation of PTTh-N/α-Fe_2O_3 photoanodes

0.004 g of TTh-N (0.3 mM) was dissolved in 30 mL dichloromethane containing 1.162 g of tetrabutylamine hexafluorophosphate (0.1 M). The solution was degassed by Ar for 25 min before polymerization. The electro-polymerization was performed on a CHI 760e electrochemical workstation at 25 °C in a three-electrode system with a platinum mesh as the counter electrode, a saturated Ag/AgCl as the reference electrode, and an α-Fe_2O_3 photoanode as the working electrode. The PTTh-N film was slowly deposited on the surface of the α-Fe_2O_3 photoanode during the cyclic voltammetry (CV) processes, in which 5 cycles were operated in a range of 0 to 2.5 V vs. $E_{Ag/AgCl}$ with a scan rate of 30 mV s^{-1}. The prepared PTTh-N/α-Fe_2O_3 samples were rinsed with dichloromethane and dried under nitrogen.

Preparation of Co@PTTh-N/FTO, Co@α-Fe_2O_3 and Co@PTTh-N/α-Fe_2O_3 electrodes

The PTTh-N/FTO electrode was prepared by the same method to the PTTh-N/α-Fe_2O_3 electrode. The prepared PTTh-N/FTO, α-Fe_2O_3 and PTTh-N/α-Fe_2O_3 electrodes were immersed in an aqueous solution of 0.1 M $Co(CH_3COO)_2$ for 30 min. After washing with deionized water, this procedure led to the generation of Co@PTTh-N/FTO, Co@α-Fe_2O_3 and Co@PTTh-N/α-Fe_2O_3 electrodes.

Mott-Schottky Analysis

The Mott-Schottky tests were conducted in 0.1M PBS solution with an AC amplitude of 5 mV at a continuously applied potential from −0.6 V to 0.6 V vs. Ag/AgCl with frequencies of 1000 Hz. The flat band potential (E_{fb}) can be calculated according to the following equation:

$$\frac{1}{C^2} = -\frac{2}{\varepsilon\varepsilon_0 A^2 e N_A}\left(E - E_{fb} - \frac{k_B T}{e}\right) \qquad \textit{eqn. S1}$$

Where ***A*** and ***C*** represent the area and interfacial capacitance, ***E*** is the applied voltage, N_A is the doping content, **e**, ***T*** and K_B are electron charge, thermodynamic temperature and Boltzmann's constant, respectively. Usually, the third term in the formula could be negligible; hence, a plot of $1/C^2$ against ***E*** could be obtained, and the E_{fb} can be determined from the intercept on the ***E*** axis.

Electrochemical Measurements

All electrochemical tests were performed on a CHI 760e electrochemical workstation in a three-electrode system with a platinum mesh as the counter electrode, an Ag/AgCl as the reference electrode and the Co@PTTh-N/FTO as the working electrode. A 0.1 M phosphate-buffered saline (PBS, pH 7.0) solution was used as the electrolyte. Unless specified, all CV was tested with a scan rate of 50 mV s^{-1}, the equation of $E_{NHE} = E_{Ag/AgCl} + 0.195$ was used to convert the potentials into normal hydrogen electrode (NHE) scale.

Turn Over Frequency (TOFs)

The TOF of the electrochemical active Co for Co@PTTh-N/FTO was calculated by ***eqn. S1***:

$$TOF = \frac{JA}{4F\Gamma A} \qquad \textit{eqn. S2}$$

Where ***J*** is water oxidation current density (A cm^{-2}) corresponding in CV curve with a lower scan rate, ***A*** is the surface area in measurement (cm^2), ***F*** is Faradaic constant (96485 C mol^{-1}). ***Γ*** is the amount of electrochemical active Co (mol cm^{-2}), which can be calculated from the inductively coupled plasma optical emission spectrometer (ICP-OES) measurement.

Photo-electrochemical Measurements

All photoelectrochemical measurements were carried out on a CHI 760e electrochemical workstation. The catalytic performance of photoanodes was evaluated in a typical three-electrode configuration with the prepared photoanodes (1×1 cm^2) as the working electrode, a platinum mesh as the counter electrode and a Ag/AgCl as the reference electrode in 0.1 M PBS (pH 7.0) solution as electrolyte. The simulated solar illumination was obtained by a 300 W Xenon arc lamp (EXCELITAS, PE300BFA) equipped with an AM 1.5G filter. The irradiation intensity of the light was adjusted to 100 mW cm^{-2} by a Newport OMM-6810B photometer (OMH-6742B, Silicon detector, 350-1100 nm). Photocurrent-potential curves were recorded by LSV with a scan rate of 10 mV s^{-1}. The recorded potential was converted into a reversible hydrogen electrode (RHE) according to the equation $E_{RHE} = E_{Ag/AgCl} + 0.195 + 0.059pH$.

Applied bias photon-to-current efficiency (ABPE)

ABPE was obtained by converting the LSV curves from ***Fig. 3a*** in the main text according to ***eqn. S2.***

$$ABPE = \frac{(1.23 - V_{RHE}) \times (J_{light} - J_{dark})}{P_{light}} \times 100\% \qquad \textit{eqn. S3}$$

Incident photon to current efficiency (IPCE)

IPCE was measured by using the 300 W Xenon arc lamp equipped with a monochromator. In short, the photocurrent density (J_{light}) and dark current density (J_{dark}) of the photoanode were measured at an applied potential of 1.23 V vs. RHE with a controlled active area (1×1 cm^2). The intensity of each monochromatic light (P_λ) at a given wavelength (λ) was recorded by a photometer (Newport OMM-6810B). According to ***eqn. S3,*** the IPCE values can be calculated.

$$IPCE = \frac{1240 \times (J_{light} - J_{dark})}{\lambda \times P_\lambda} \times 100\% \qquad \textit{eqn. S4}$$

Photoelectrochemical impedance spectroscopy (PEIS)

Nyquist plots were performed with a bias potential at 1.1 V vs RHE under 100 mW cm^{-2} light illumination. The frequency range was set between 100 kHz to 0.1 Hz with an amplitude frequency of 10 mV.

Surface charge separation efficiency ($\eta_{surface}$)

The surface charge separation efficiency ($\eta_{surface}$) was calculated using the ***eqn. S5***.

$$\eta_{surface} = \frac{J_{H_2O}}{J_{hs}} \qquad \textit{eqn. S5}$$

Where J_{hs} is the photocurrent density of the sample with hole scavenger, J_{H2O} is the photocurrent density in a buffer.

Faradaic efficiency

The amount of oxygen evolution from the photoelectrochemical reaction was determined by gas chromatography (Techcomp GC 7890T, Ar carrier gas, Thermo

Conductivity Detector). The potentiostatic method (at 1.23 V vs RHE) was used to electrochemical and photoelectrochemical measurements. The theoretical O_2 evolution can be calculated by the amount of charge passed through electrodes.

$$FE(\%) = \left(\frac{4eN_A n_{O_2}}{Q}\right) \times 100\% \qquad \textit{eqn. S6}$$

Where ***e*** is the elementary charge, $\boldsymbol{N}_A$ is the Avogadro constant, $\boldsymbol{n}_{O2}$ is the amount of oxygen determined by gas chromatography, and ***Q*** is the integrated charge passed through the photoelectrodes.

Photoluminescence spectroscopy (PL)

PL was conducted by steady state transient fluorescence spectrometer (FluoroMax-4P) with an excitation wavelength of 400 nm.

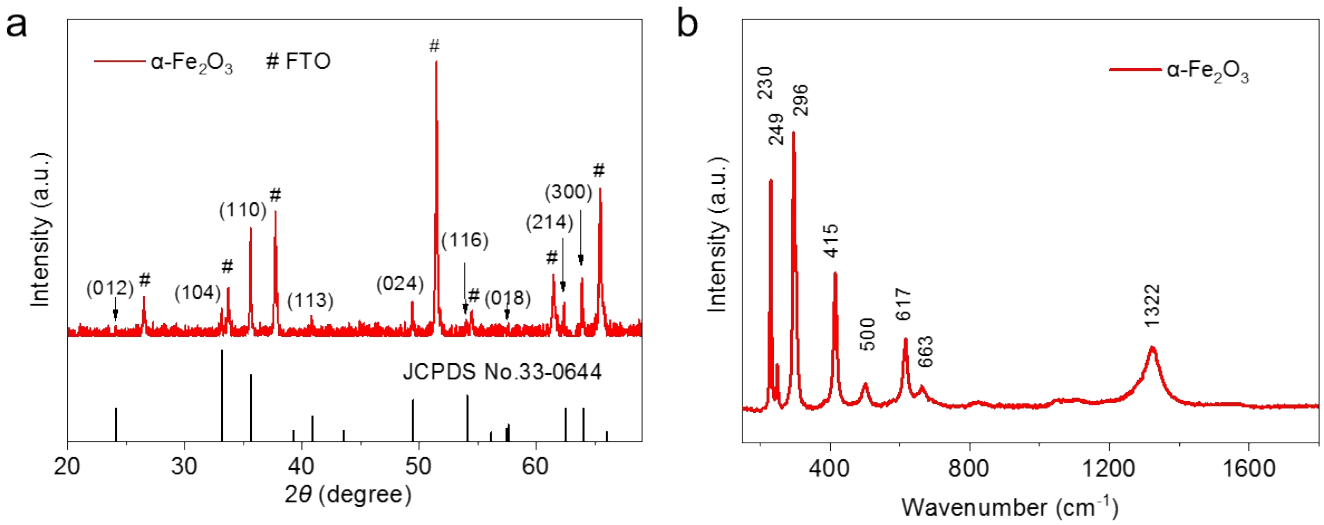

Figure S4. (a) XRD pattern and (b) Raman spectrum of α-Fe_2O_3 photoanode.

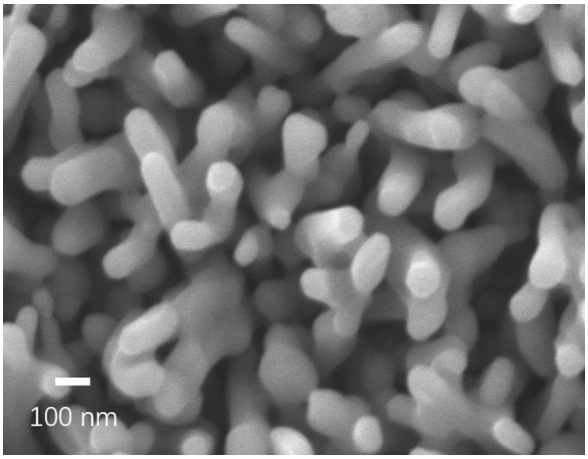

Figure S5. SEM image of α-Fe_2O_3 photoanode.

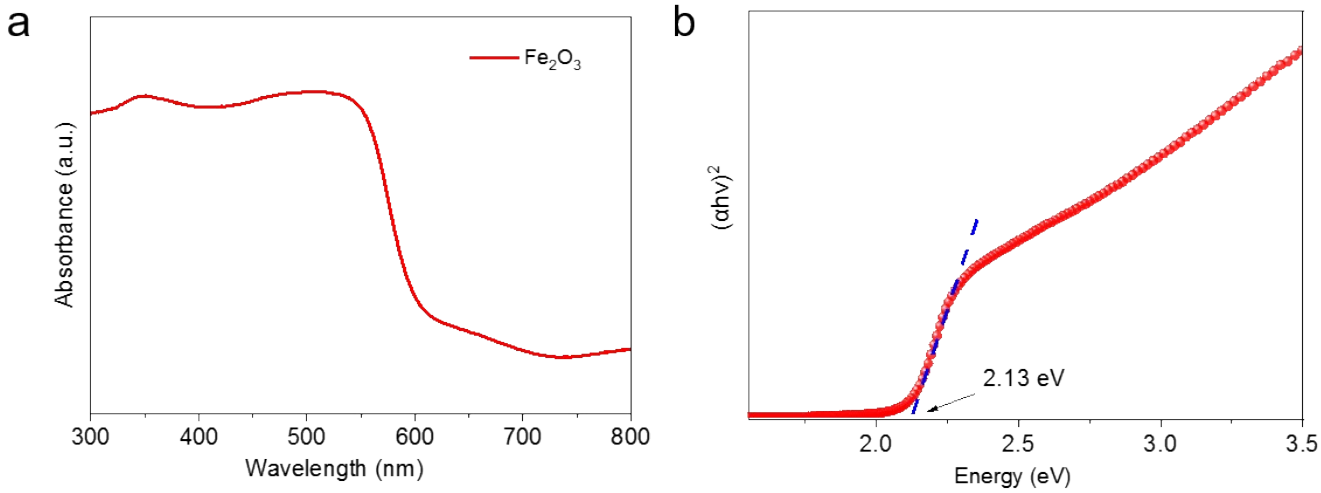

Figure S6. (a) UV-vis absorbance spectrum and (b) Tauc plot of α-Fe_2O_3 thin film. The bandgap of α-Fe_2O_3 is determined to be 2.13 eV.

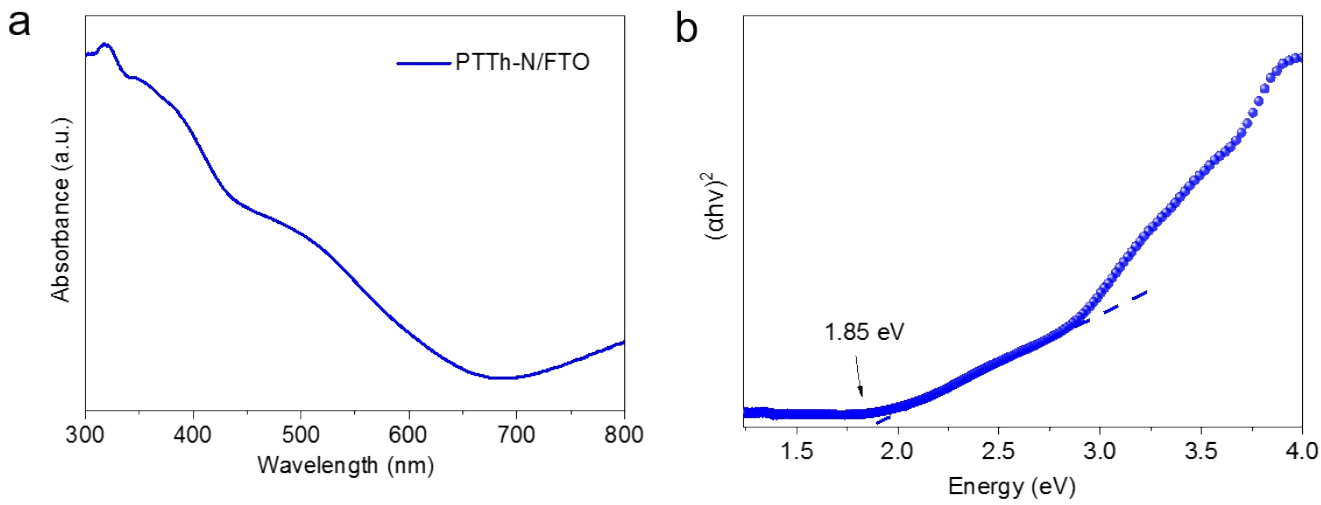

Figure S7. (a) UV-vis absorbance spectrum and (b) Tauc plot of PTTh-N reference thin film. The bandgap of PTTh-N is determined to be 1.85 eV.

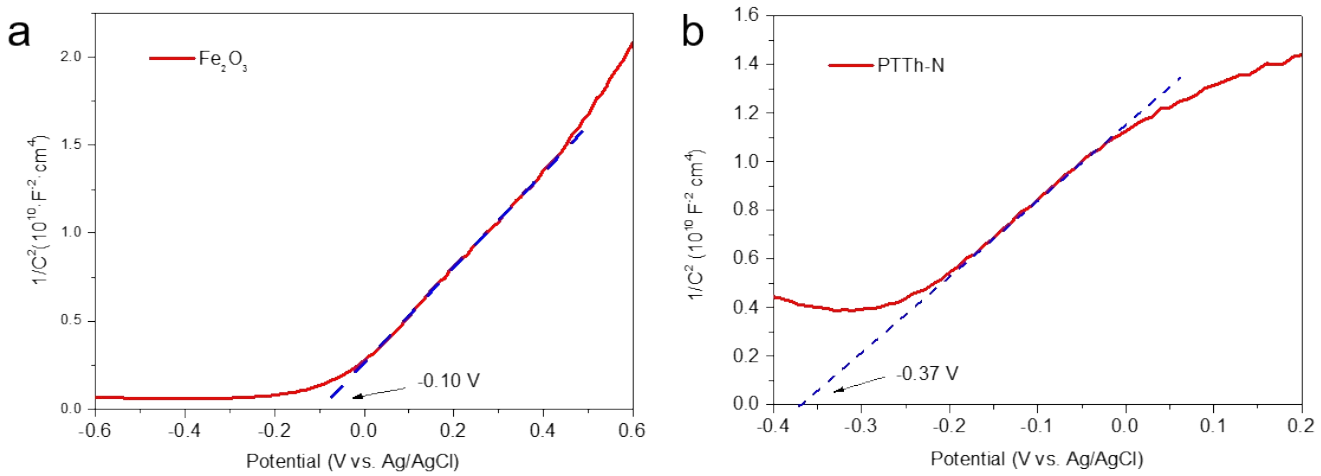

Figure S8. Mott-Shottky plots of (a) α-Fe_2O_3 and (b) PTTh-N film on FTO.

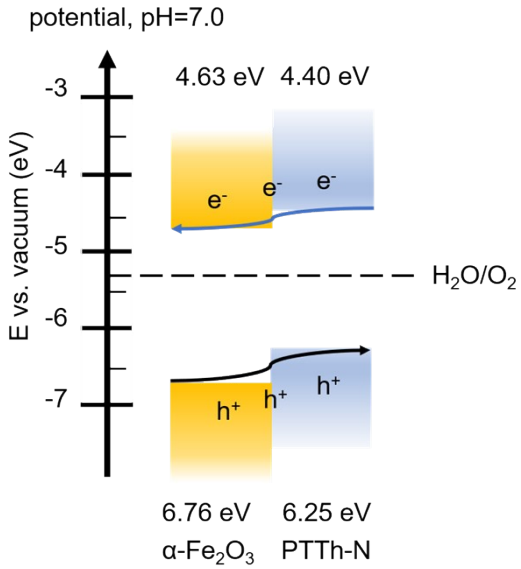

Figure S9. The band alignment diagram of the PTTh-N/α-Fe_2O_3 photoanode.

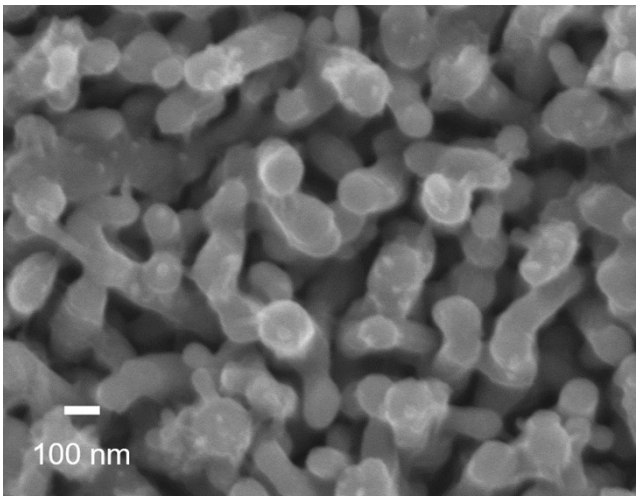

Figure S10. SEM image of PTTh-N/α-Fe_2O_3 photoanode.

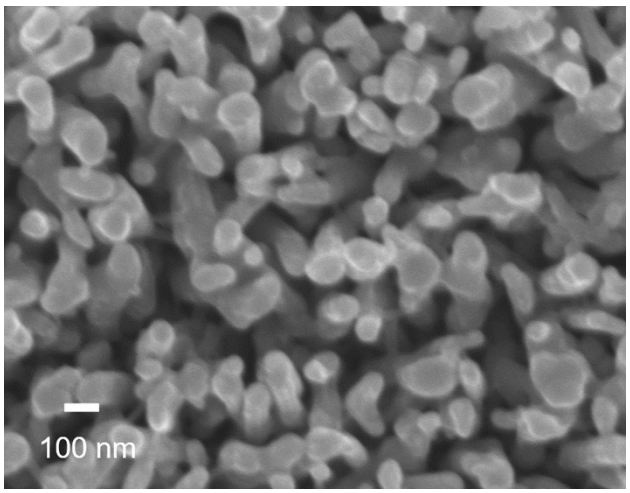

Figure S11. SEM image of Co@PTTh-N/α-Fe_2O_3 photoanode.

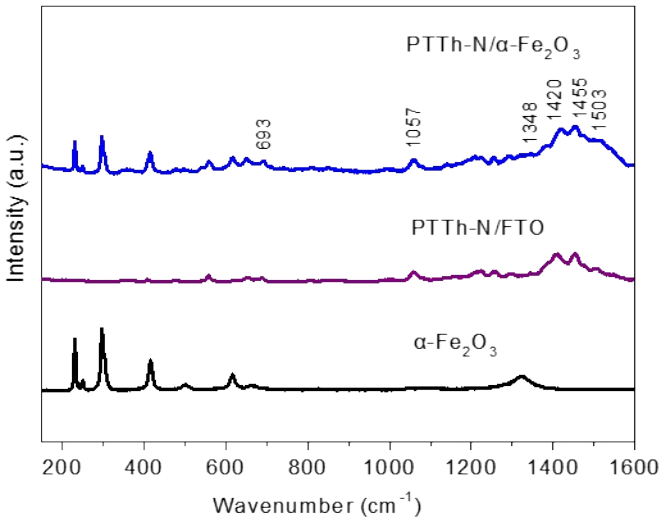

Figure S12. Raman spectra of α-Fe_2O_3, PTTh-N/FTO and PTTh-N/α-Fe_2O_3.

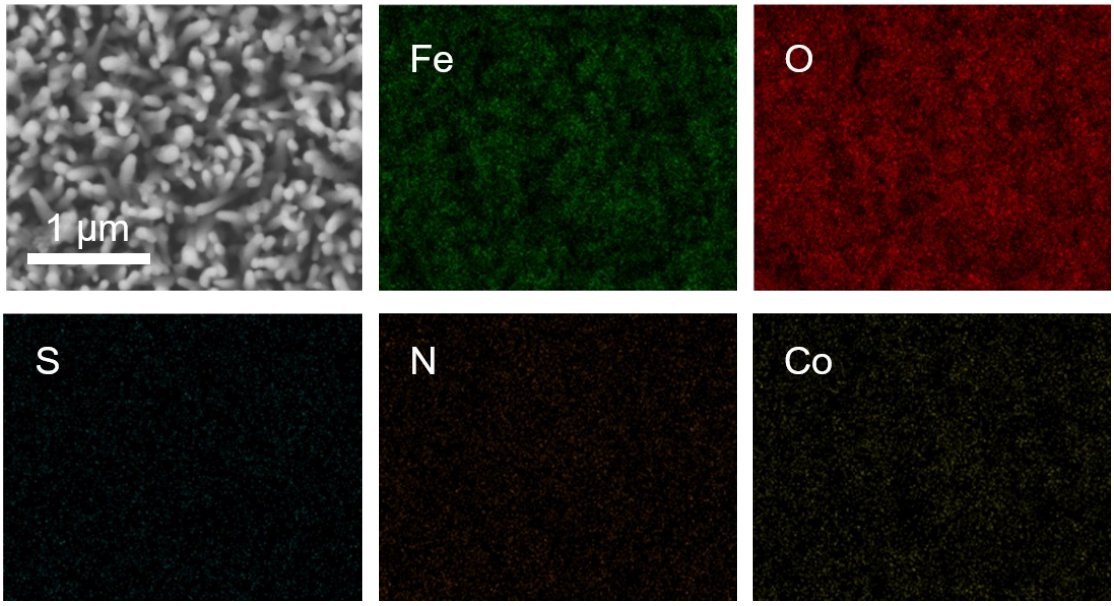

Figure S13. Top view SEM image of the Co@PTTh-N/α-Fe_2O_3 photoanode with corresponding elemental mapping images.

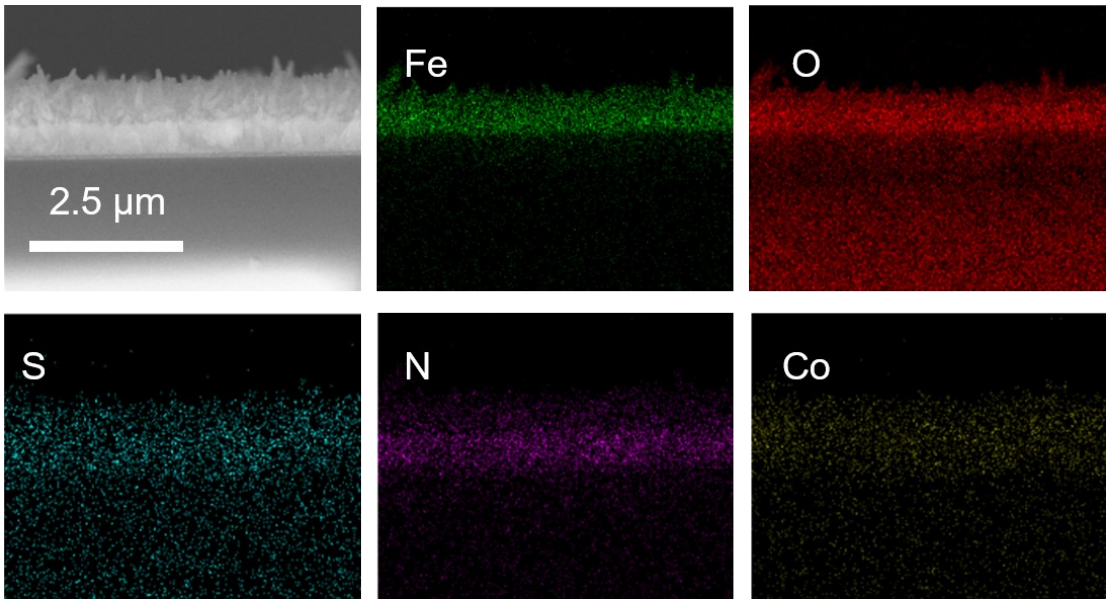

Figure S14. Cross-sectional view SEM image of the Co@PTTh-N/α-Fe_2O_3 photoanode with corresponding elemental mapping images.

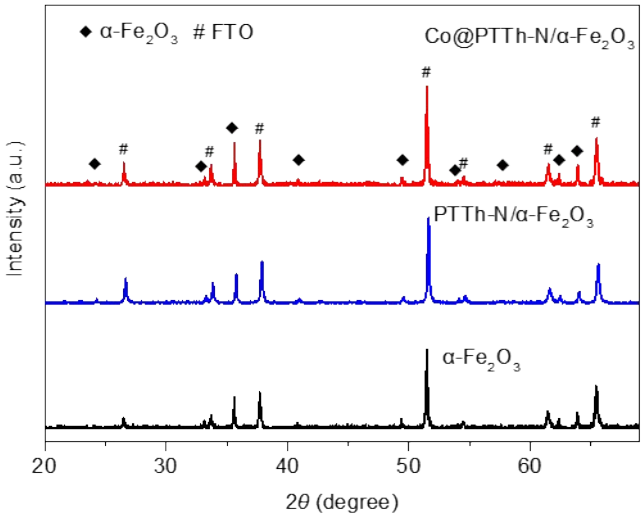

Figure S15. XRD patterns of the α-Fe_2O_3, PTTh-N/α-Fe_2O_3 and Co@PTTh-N/α-Fe_2O_3 photoanodes.

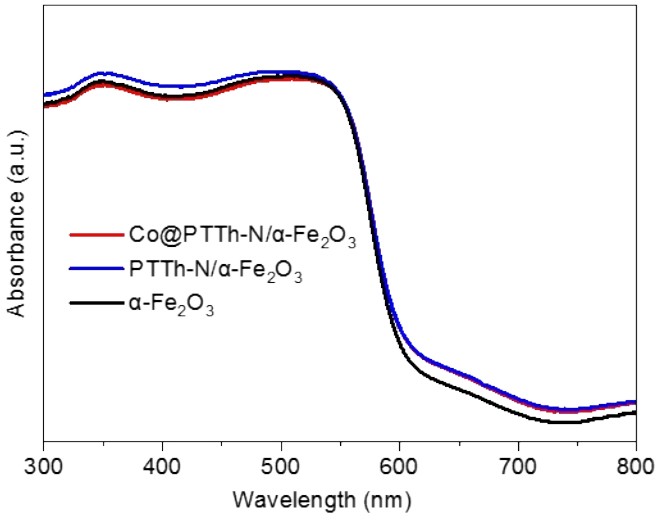

Figure S16. UV-Vis diffuse spectra of α-Fe_2O_3, PTTh-N/α-Fe_2O_3 and Co@PTTh-N/α-Fe_2O_3 photoanodes.

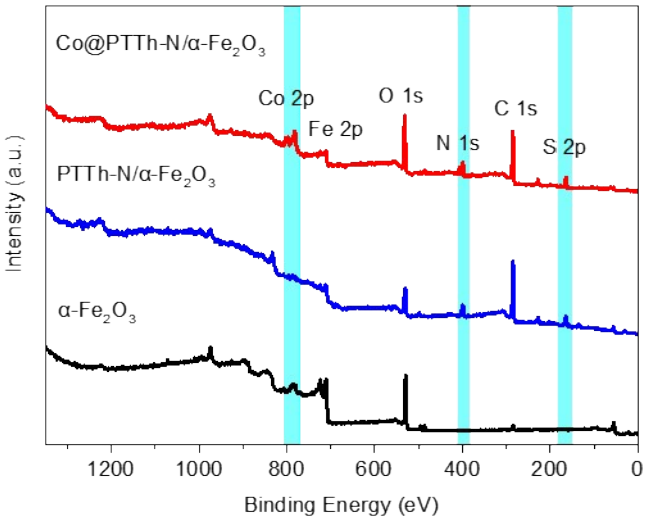

Figure S17. XPS survey spectra of α-Fe_2O_3, PTTh-N/α-Fe_2O_3 and Co@PTTh-N/α-Fe_2O_3 photoanodes.

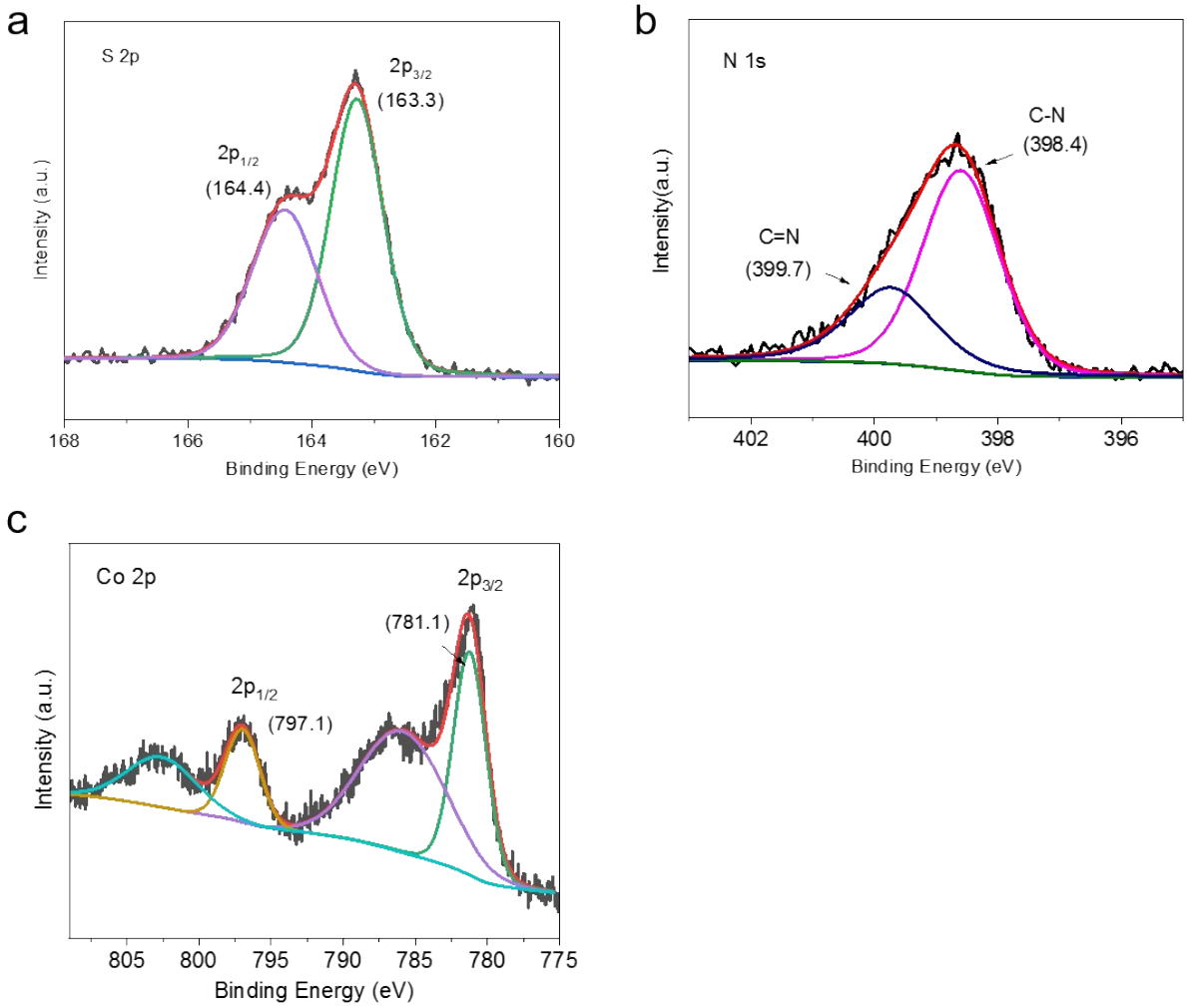

Figure S18. High-resolution XPS spectra of the Co@PTTh-N/α-Fe_2O_3 photoanode in selected (a) S 2p, (b) N 1s and (c) Co 2p regions.

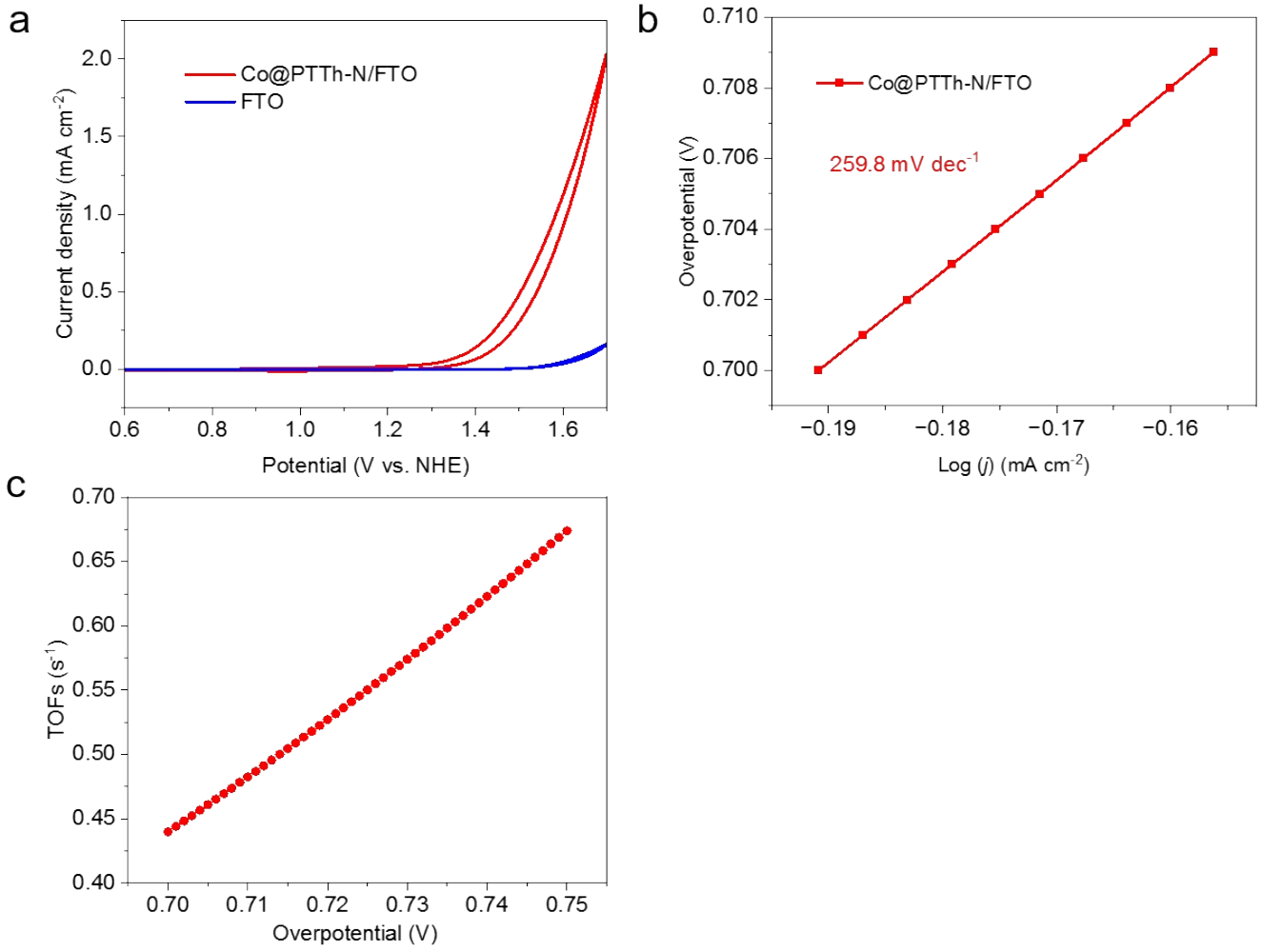

Figure S19. (a) CV measurements of the Co@PTTh-N/FTO electrode in 0.1 M PBS (pH 7.0) at a scan rate at 50 mV s^{-1} without iR compensation. (b) Tafel plots of Co@PTTh-N/FTO. (c) TOFs of Co@PTTh-N/FTO electrode based on the Co^{2+} loading (calculated according to ICP-OES) and current densities vs. various overpotentials.

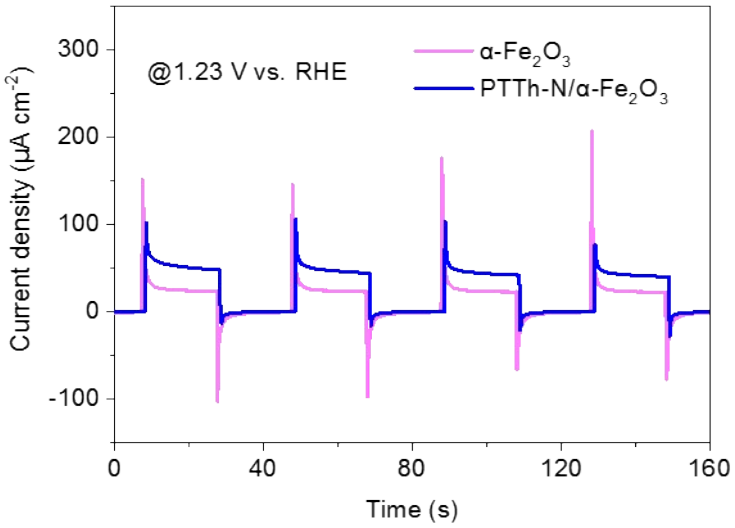

Figure S20. Current density-time curves of α-Fe_2O_3 and PTTh-N/α-Fe_2O_3 photoanodes under chopped illumination (AM 1.5 G,100 mW cm^{-2}).

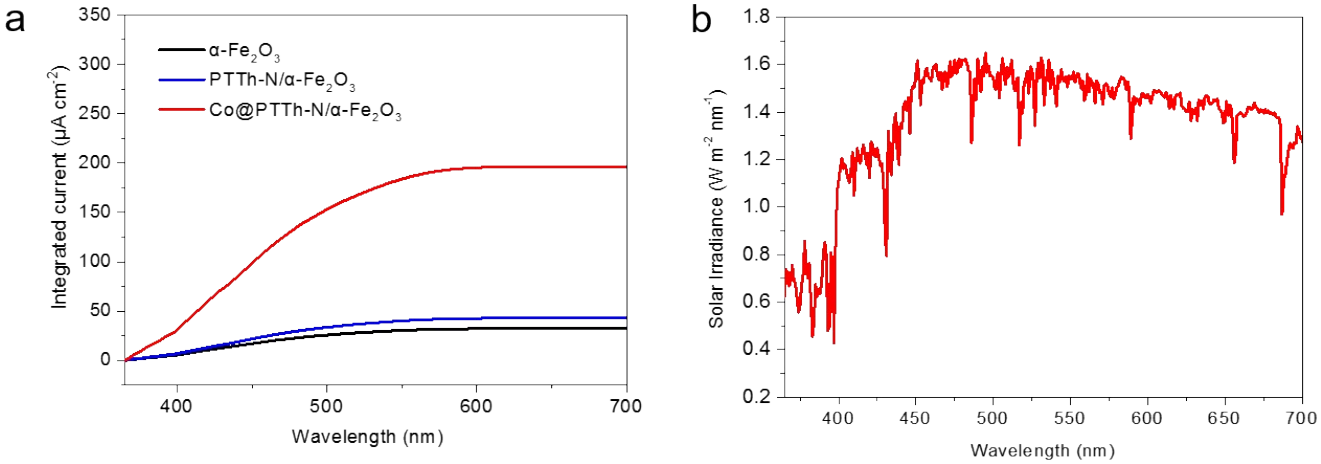

Figure S21. (a) Solar irradiance of AM 1.5G (ASTM G173-03) and (b) Calculated photocurrent of α-Fe_2O_3, PTTh-N/α-Fe_2O_3 and Co@PTTh-N/α-Fe_2O_3 photoanodes by integrating IPCE at 1.23 V vs. RHE over the photon flux of AM 1.5G.

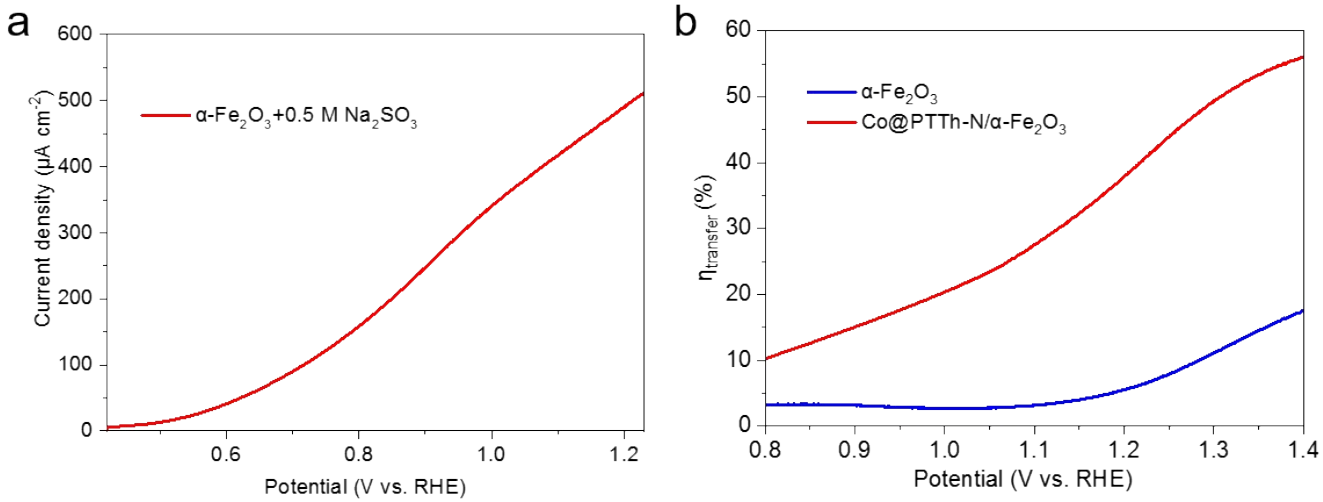

Figure S22. LSV curve of α-Fe_2O_3 photoanode under continuously illumination (AM 1.5 G,100 mW cm^{-2}) in 0.1 M PBS with 0.5 M Na_2SO_3; (b) Surface charge transfer efficiency of α-Fe_2O_3 and Co@PTTh-N/α-Fe_2O_3 photoanodes.

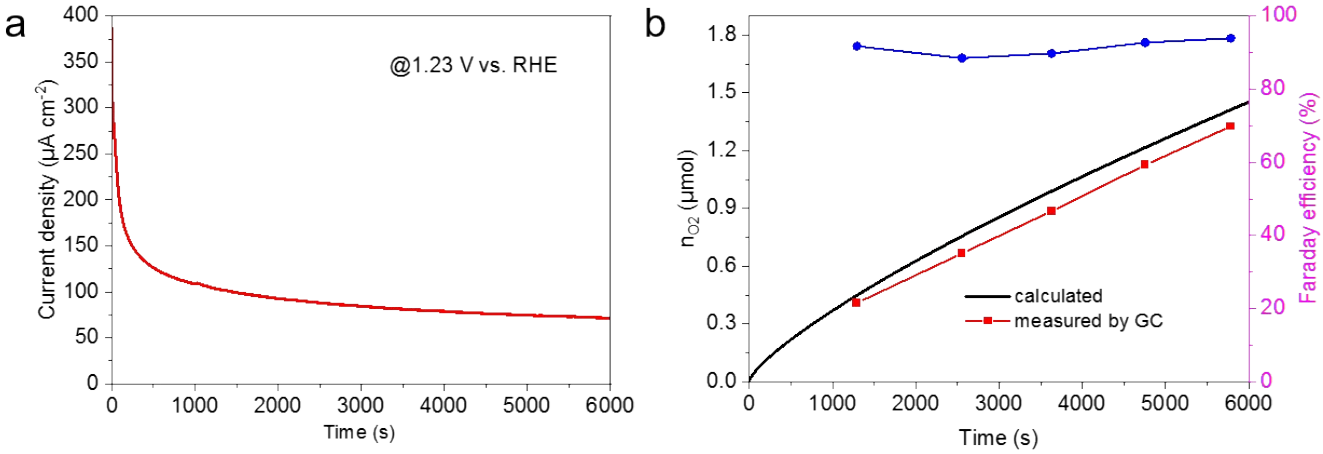

Figure S23. (a) i-t curve of Co@PTTh-N/α-Fe_2O_3 photoanode at a constant applied potential of 1.23 V vs. RHE. Measurement was carried out in a 0.1 M PBS (pH 7.0) under AM 1.5G simulated sunlight irradiation (100 mW cm^{-2}); (b) Faradaic efficiency of Co@PTTh-N/α-Fe_2O_3 photoanode for OER. Oxygen evolution detected by gas chromatography and the charge passed during the photolysis of Co@PTTh-N/α-Fe_2O_3 photoanode at an applied potential of 1.23 V vs. RHE.

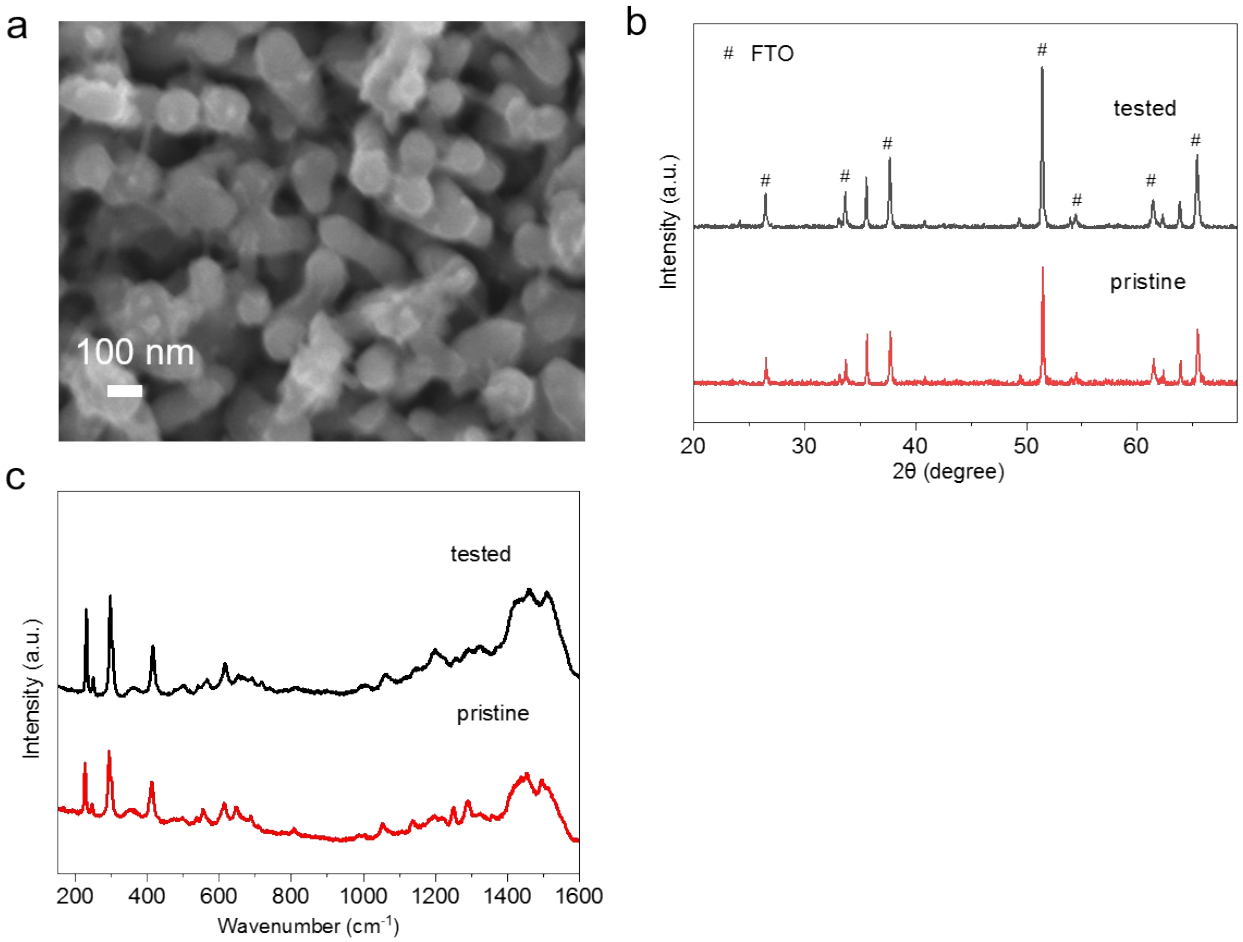

Figure S24. (a) SEM image, (b) XRD pattern and Raman spectrum of tested Co@PTTh-N/α-Fe_2O_3 photoanode.

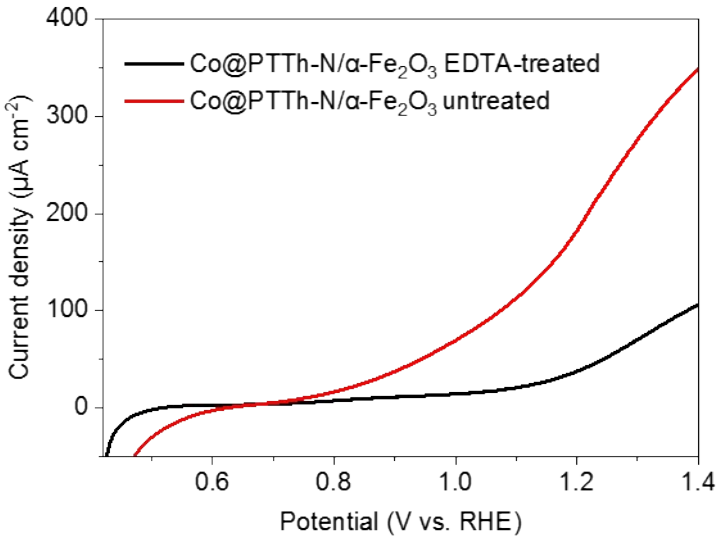

Figure S25. LSV curves of EDTA-treated and untreated Co@PTTh-N/α-Fe_2O_3 photoanodes.

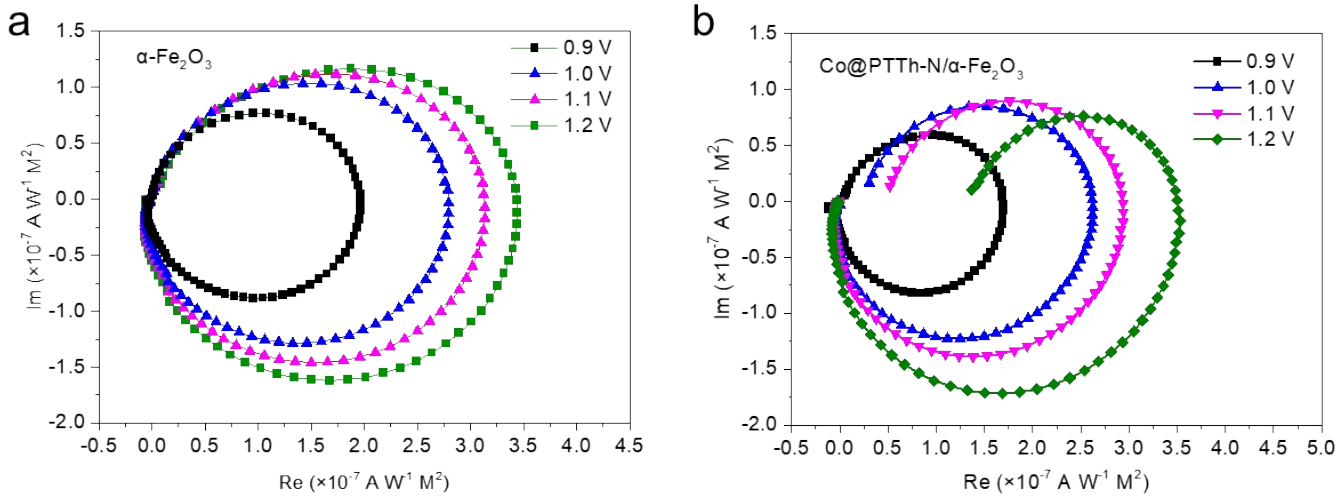

Figure S26. IMPS spectra of (a) α-Fe_2O_3 and (b) Co@PTTh-N/α-Fe_2O_3 photoanodes at different applied potentials.

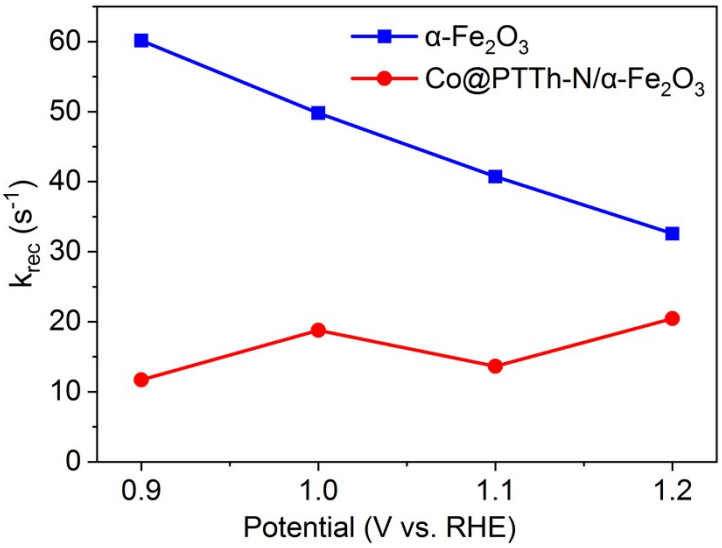

Figure S27. Rate constant of charge recombination (k_{rec}) of α-Fe_2O_3 and Co@PTTh-N/α-Fe_2O_3 photoanodes.

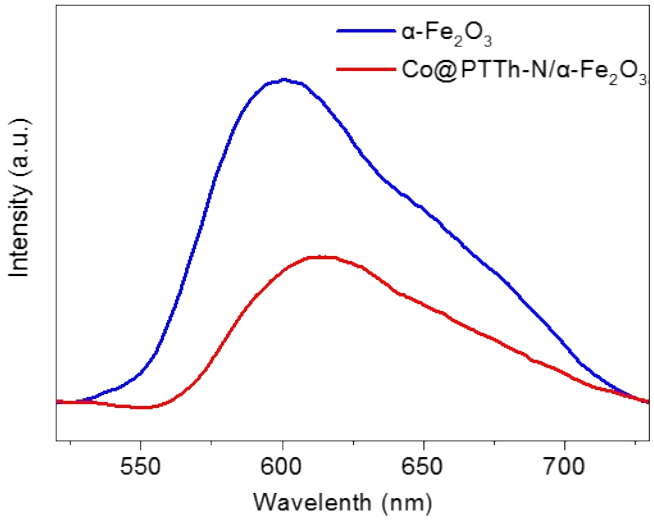

Figure S28. PL spectra of α-Fe_2O_3 and Co@PTTh-N/α-Fe_2O_3 photoanodes.

Table S1 The values of fitting parameters for PEIS tests

	R_s (Ω)	R_{SC} (Ω)	R_{ct} (Ω)	C_{SC} ($\times10^{-5}$ F)	C_h ($\times10^{-4}$ F)
α-Fe_2O_3	42.9	276.1	8816	2.8	2.8
Co@PTTh-N/α-Fe_2O_3	44.7	227.3	767	4.1	2.9

References

1. J.-i. Nishida, S. Murakami, H. Tada and Y. Yamashita, *Chemistry Letters*, 2006, **35**, 1236-1237.

2. Y. Yang, M. Forster, Y. Ling, G. Wang, T. Zhai, Y. Tong, A. J. Cowan and Y. Li, *Angewandte Chemie International Edition*, 2016, **55**, 3403-3407.